physica status solidi rrl
www.pss-rapid.com

Transition Metals in a Cast-Monocrystalline Silicon Ingot Studied by Silicon Nitride Gettering

Chang Sun, AnYao Liu, Aref Samadi, Catherine Chan, Alison Ciesla, and Daniel Macdonald*

The concentrations of Cr, Fe, Ni, and Cu in a cast-monocrystalline silicon ingot grown for solar cell applications are reported. Wafers taken from along the ingot are coated with silicon nitride films and annealed, causing mobile impurities to be gettered to the films. Secondary ion mass spectrometry is applied to measure the metal content in the silicon nitride films. The bulk concentrations of the gettered metals in samples along the ingot are found to be: Cr (3.3×10^{10}–3.3×10^{11} cm^{-3}), Fe (3.2×10^{11}–2.5×10^{12} cm^{-3}), Ni (1.5×10^{12}–1.3×10^{13} cm^{-3}), and Cu (7.1×10^{11}–3.2×10^{13} cm^{-3}). For each metal, the lower limit is measured on the wafer from the middle of the ingot, and the higher limit is measured on wafers from the bottom or the top. The results are compared with similar data recently measured on a high-performance multicrystalline silicon ingot. The results provide insights into the total bulk concentrations of the metals in cast-grown ingots.

Metallic impurities are commonly found in photovoltaic-grade silicon materials. They reduce the carrier lifetime of silicon materials in both the dissolved state and the precipitated state, and are thus detrimental to silicon solar cells.[1–3] Knowledge of the metal concentrations in silicon materials is also significant for the studies of other defects, including light and elevated temperature-induced degradation,[4,5] decorated crystal defects such as dislocations and grain boundaries,[6] copper-related light-induced degradation,[7] boron-oxygen-related defects,[8,9] ring defects,[10,11] and so on. The metal concentrations in multicrystalline silicon (mc-Si) ingots have been successfully determined by applying neutron activation analysis in previous studies.[12–14] However, as the ingot growth techniques have become much cleaner in recent years, some of the previous data are out of date. In a recent study,[15] metals in the bulk of high-performance (HP) mc-Si wafers were gettered into thin layers on the surface, and the gettered concentrations were determined by applying secondary ion mass spectrometry (SIMS) analysis. In this approach, a key factor is concentrating the metals into thin surface layers, as the bulk concentrations are usually below the detection limits of the SIMS analysis. The gettered concentrations were found to be 3–4 orders of magnitude higher than those in the bulk (depending on the thickness of the wafer and films).[15,16] Ref. [15] also compared the gettering efficiencies of plasma-enhanced chemical vapor-deposited (PECVD) SiN_x films and typical phosphorus diffusion gettering, and showed that the SiN_x film is an effective gettering layer for metal impurities.[16] In this work, we will apply this approach to a cast-grown monocrystalline-like (cast-mono) Si ingot, and use the SiN_x film as the gettering layer.

The wafers were from a B-doped p-type cast-mono silicon ingot cut from the central part of the original ingot provided by ECM Greentech. In comparison with the edge of the original ingot, lower concentrations of impurities might be expected in the central part considering the in-diffusion of impurities from the crucible.[13] Six 15.6 × 15.6 cm wafers from different solidified fractions g in the range of 0.23–0.79 were chosen for this study. The corresponding doping levels [B] were in the range of 9.7×10^{15} to 1.2×10^{16} cm^{-3}, as determined by dark conductance measurements. Two 4 × 4 cm square wafers were cut from two corners of each large wafer using a laser cutter. The small wafers were divided into two groups: the lifetime group included one small wafer from each solidified fraction (six wafers), while only three wafers, from the bottom ($g = 0.23$), middle ($g = 0.54$), and top ($g = 0.79$), were included in the SIMS group. All nine wafers were saw damage-etched. The thickness W of the wafers after etching was 180–190 μm. Then they were RCA-cleaned (including HP dips after each of RCA1 and RCA2), followed by the deposition of a 70-nm PECVD SiN_x film on each side, in a Roth and Rau AK400 chamber. The temperature of the sample stage during deposition was about 300 °C. More details of the deposition process can be found in Ref. [16].

After passivation, the dissolved interstitial Fe and Cr concentrations ($[Fe_i]$ and $[Cr_i]$) in the wafers in the lifetime group were determined with the following procedure: a) The wafers were kept at 53 °C in the dark on a hotplate for >3 days to fully associate both FeB and CrB pairs,[17,18] before the lifetime τ_{assoc} was measured using a Sinton Instruments WCT-120 quasi-steady-state

Dr. C. Sun, Dr. A. Y. Liu, Prof. D. Macdonald
Research School of Electrical, Energy & Materials Engineering
The Australian National University
Canberra, ACT 2601, Australia
E-mail: chang.sun@anu.edu.au

A. Samadi, Dr. C. Chan, Dr. A. Ciesla
School of Photovoltaic and Renewable Energy Engineering
University of New South Wales
Kensington, NSW 2052, Australia

The ORCID identification number(s) for the author(s) of this article can be found under https://doi.org/10.1002/pssr.201900456.

DOI: 10.1002/pssr.201900456

photoconductance lifetime tester. b) A flashlight was used to illuminate the samples to fully dissociate the FeB pairs, and the lifetime was measured. The illumination does not dissociate CrB pairs.[18] This lifetime measured after illumination, where FeB pairs were fully dissociated but CrB pairs were fully associated, was denoted as τ_{ls}. $[Fe_i]$ was determined using $[Fe_i] = C_1(1/\tau_{assoc} - 1/\tau_{ls})$,[19] with the recombination parameters of Fe_i and FeB taken from Ref. [20]. c) The wafers were then annealed at 260 °C in the dark for 8 min and subsequently quenched in cold water. This process can effectively dissociate >95% CrB pairs in all the wafers.[18] After quenching, the samples were illuminated again with the flashlight for a short time to make sure that the FeB pairs remain dissociated, before the lifetime τ_{quench} was measured. The predicted CrB dissociation fraction f_{dissoc} was taken into account when calculating $[Cr_i]$ using $[Cr_i] = C_2(1/\tau_{ls}–1/\tau_{quench})/f_{dissoc}$.[21] The recombination parameters of Cr_i and CrB were taken Ref. [18].

SiN_x gettering was then performed on all the wafers from both groups. They were RCA-cleaned (without HF dips to keep the SiN_x films) and annealed at 700 °C for 90 min in N_2 in a highly clean quartz tube furnace. The samples were loaded and unloaded at 700 °C, and were cooled down in air after unloading. The temperature and duration were chosen to allow >99% Cr_i (which has a lower diffusivity compared with Fe_i, Ni_i, and Cu_i), to move to the surfaces.[1,15] Note that as confirmed in previous works,[15,16] the preparation or gettering process of the samples does not introduce extra contamination that can be detected by SIMS. After gettering, SIMS measurements were conducted on the three wafers from the SIMS group to determine the concentrations of Cr, Fe, Ni, and Cu in the SiN_x film and the silicon bulk near the interface as a function of depth. The SIMS measurements were conducted by Evans Analytical Group Laboratories, and greater detail can be found in the previous studies.[15,16] The step size of data collection was 1.4–1.8 nm. The data collection area is a circle with 60 μm in diameter for Cr and Fe, and 30 μm in diameter for Ni and Cu. For the wafer from the top that is more mc-Si-like, defective areas with large densities of dislocations and highly-concentrated metals were observed during the measurement, and were avoided, to ensure the repeatability of the analyses. For the wafers in the lifetime group, the annealed SiN_x films were removed due to the lost passivation effects after annealing, and fresh SiN_x films were deposited. The thermal budget of the re-passivation process was negligible compared with gettering annealing. The lifetime was then measured when FeB and CrB were fully associated.

Figure 1 shows the lifetimes measured before and after gettering. Improvements of lifetime were observed on all the wafers, indicating reduced concentrations of impurities in the bulk. The improvements were more pronounced in wafers from the bottom and top than those from the middle.

The results of SIMS measurements are shown in **Figure 2**. The SiN_x film and silicon bulk were differentiated by monitoring the raw ion counts. The detection limits for the metals in both silicon and SiN_x are shown in the figure. A steep decrease in concentrations in the first 40–50 nm was related to unwanted surface contamination.[16] Following a steep decrease, the concentration peaks around the SiN_x/Si interface corresponded to the metals gettered to the interface. The mechanism of aggregation of the metals at

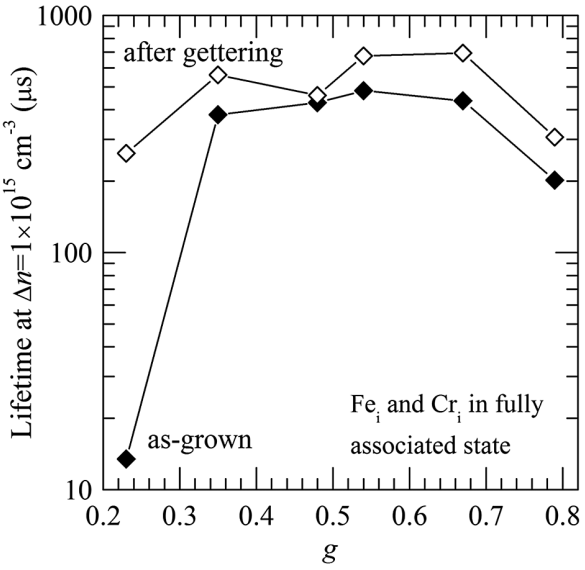

Figure 1. Lifetime at $\Delta n = 1 \times 10^{15}$ cm^{-3} before and after SiN_x gettering, as a function of solidified fraction g. Fe_i and Cr_i were in the associated state during measurements.

the interface is not fully understood at this stage, but is likely a segregation gettering mechanism.[16,22] The result that the metals were gettered to the interface is consistent with what was observed on HP mc-Si wafers in Ref. [15]. However, in Ref. [16] where Fe was the only main contaminant in the wafers, Fe was gettered to the bulk of the SiN_x films during annealing. As speculated in Ref. [15] the preferential gettering sites of the metals might be affected by the difference in the amounts of gettered metals, and the interaction of multiple metals during precipitation. In silicon, both fast diffusers, Cu and Ni, can precipitate via a homogeneous nucleation mechanism at the interface.[1] The precipitates act as a further diffusion source into the SiN_x film, and also form nuclei for other impurities, including Fe and Cr, which usually tend to precipitate via a heterogeneous nucleation mechanism.[1] This co-precipitation behavior of the metals may explain why Fe precipitates at the interface only when certain amounts of Cu or Ni are present. The reason why Cu and Ni did not precipitate uniformly in the bulk of the SiN_x films could be partly attributed to the orders of magnitudes of lower diffusivities in SiN_x than in Si.[23,24]

Each depth profile in Figure 2 was then integrated with respect to the depth to obtain the metal concentration that was gettered to the interface on one side (in cm^{-2}), $[M_{interface}]$, with the method described in Ref. [15]. Both the artifacts near the surface and data below the detection limits were disregarded in this method. As the metals should be equally gettered to both surfaces of a wafer, the bulk concentration (in cm^{-3}) of the total gettered metal, $[M_{gettered}]$, was then obtained using $[M_{gettered}] = [M_{interface}] \times 2/W$. The results of $[M_{gettered}]$ are summarized in **Figure 3**, together with $[Cr_i]$ and $[Fe_i]$ in as-cut wafers determined based on lifetime measurements. As $[Cr_i]$ in most wafers was too low to be determined, only the maximum values that consider 5% relative error in the measured lifetimes are shown in the figure. $[Fe_i]$ was found to be lower compared with those reported in the previous

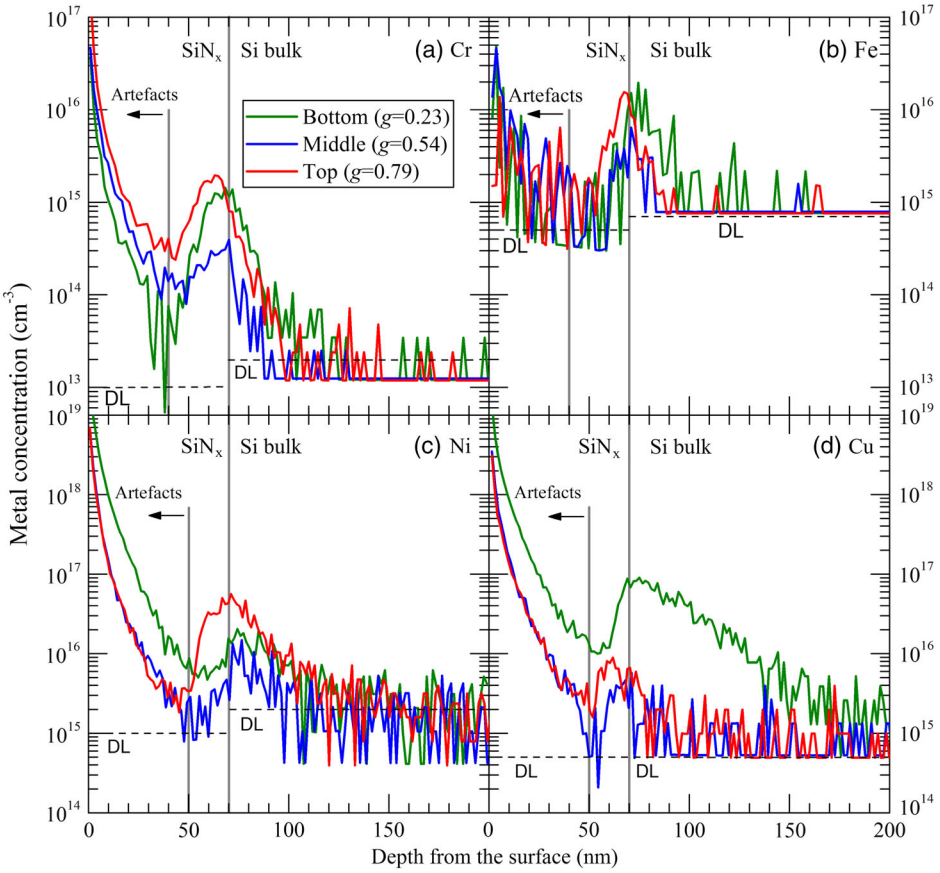

Figure 2. SIMS depth profiles of a) Cr, b) Fe, c) Ni, and d) Cu, in wafers from the bottom, middle, and top of the cast-mono ingot. The wafers were passivated with 70-nm SiN_x films on both sides before gettering annealing.

studies.[25,26] The data measured on an HP mc-Si ingot from Ref. [15] are also shown for comparison. The data were measured in the intra-grain regions of mc-Si wafers. Note that Ref. [15] showed the gettered metal concentrations to the SiN_x film *on one side*; the concentrations were doubled and are shown in Figure 3.

As shown in the figure, the gettered metal concentrations and [Fe_i] in the as-cut wafers were mostly very comparable in both ingots. For the HP mc-Si ingot, some data points at the bottom and middle parts of the ingot were missing because the metal concentration was below the detection limit in these cases.[15] In fact, the high concentrations of crystal defects, such as grain boundaries, in HP mc-Si wafers reduced the gettered metal concentrations measured by SIMS because: a) the crystal defects act as internal gettering sites for the metals,[12] and thus reduce the concentrations gettered externally by the interface and SiN_x films; b) crystal defect-rich regions with highly concentrated metals were avoided during the SIMS analysis to ensure the repeatability of results in both Ref. [15] and this work. For the same reasons, the gettered metal concentrations in the wafer from the top, where there are more crystal defects, could be reduced. Comparing different positions of the cast-mono ingot, we can see that higher concentrations of metals were gettered in the wafers from the top and bottom than those from the middle. This is consistent with the lifetime measurements shown in Figure 1. It indicates higher concentrations of metals in the as-cut wafers from the top and the bottom. The distribution of the metals along the ingot can be affected by several factors, including segregation at the solid/liquid interface during solidification, in-diffusion from the crucible, and diffusion in the solid state during ingot cooling.[13]

For both Cr and Fe, the gettered concentration was much higher than the interstitial concentration in almost all the wafers, indicating that the majority of the gettered metals were from the dissolution of precipitates. This was also expected to be the case for Ni and Cu as they were mainly precipitated in silicon at room temperature. As the dissolution of precipitates may not be complete, the gettered concentration might be only a fraction of the total bulk concentration, as discussed in the previous studies.[15,27] An exception was Fe in the bottom wafer, where [Fe_i] was very close to the gettered [Fe], indicating that Fe was mostly dissolved in this wafer before gettering. This could be caused by a low concentration of crystal defects acting as precipitation sites for Fe in this wafer.

In conclusion, SiN_x gettering was performed on wafers from along a cast-mono silicon ingot, to concentrate the metal impurities from the wafer bulk into the SiN_x films. The depth profiles of the gettered Cr, Fe, Ni, and Cu concentrations were then determined by SIMS measurements. The results showed that the metals were gettered to the SiN_x/Si interface. The bulk concentrations of the gettered metals were calculated, providing

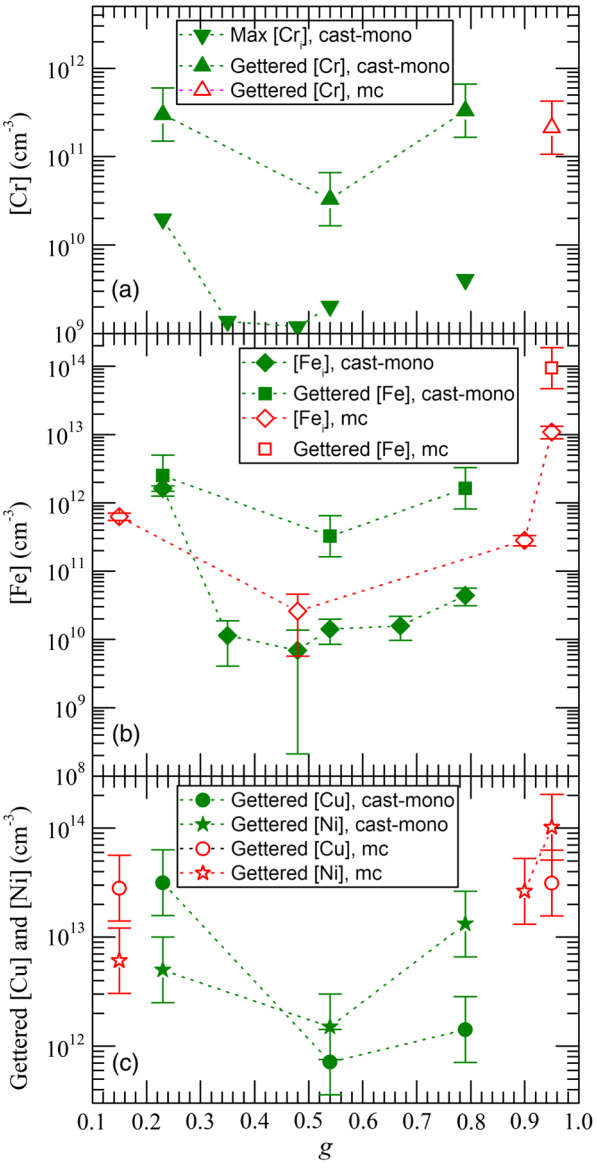

Figure 3. Bulk concentrations of a) Cr, b) Fe, c) Ni and Cu that were gettered to the SiN_x films on both surfaces. Error bars indicate the relative error (−50%, +100%) of SIMS measurement. Green, filled symbols are data of the cast-mono silicon ingot from this work. Red, open symbols are data of an HP mc-Si ingot (measured in intra-grain regions) from Ref. [15]. The maximum [Cr_i] in the cast-mono ingot that considers 5% relative error in the measured lifetime is shown in (a). [Fe_i] in as-cut samples from both ingots is shown in (b), and error bars account for 5% relative error in the measured lifetime.

insights into the total bulk concentrations and chemical state of metals in the as-grown ingot.

Acknowledgements

This work has been supported by the Australian Renewable Energy Agency (ARENA) through project 2017/RND010. A.Y.L. was supported by the ARENA ACAP Postdoctoral Research Fellowship.

Conflict of Interest

The authors declare no conflict of interest.

Keywords

cast-mono, gettering, silicon nitride, transition metals

Received: August 7, 2019
Revised: September 3, 2019
Published online:

[1] K. Graff, *Metal Impurities in Silicon-Device Fabrication*, Springer, Berlin **2000**.
[2] G. Coletti, P. C. Bronsveld, G. Hahn, W. Warta, D. Macdonald, B. Ceccaroli, K. Wambach, N. Le Quang, J. M. Fernandez, *Adv. Funct. Mater.* **2011**, *21*, 879.
[3] J. Schmidt, B. Lim, D. Walter, K. Bothe, S. Gatz, T. Dullweber, P. P. Altermatt, in *2012 IEEE 38th Photovoltaic Specialists Conf. (PVSC) PART 2*, **2012**, https://doi.org/10.1109/PVSC-Vol2.2012.6656779.
[4] C. Vargas, Y. Zhu, G. Coletti, C. Chan, D. Payne, M. Jensen, Z. Hameiri, *Appl. Phys. Lett.* **2017**, *110*, 092106.
[5] D. Bredemeier, D. C. Walter, J. Schmidt, *Sol. RRL* **2018**, *2*.
[6] H. T. Nguyen, F. E. Rougieux, F. Wang, H. Tan, D. Macdonald, *IEEE J. Photovoltaics* **2015**, *5*, 799.
[7] H. Savin, M. Yli-Koski, A. Haarahiltunen, *Appl. Phys. Lett.* **2009**, *95*, 152111.
[8] M. Kim, D. Chen, M. Abbott, N. Nampalli, S. Wenham, B. Stefani, B. Hallam, *J. Appl. Phys.* **2018**, *123*, 161586.
[9] J. Schmidt, K. Bothe, V. V. Voronkov, R. Falster, *Phys. Status Solidi B* **2019**, https://doi.org/10.1002/pssb.201900167.
[10] C. Sun, H. T. Nguyen, F. E. Rougieux, D. Macdonald, *J. Cryst. Growth* **2017**, *460*, 98.
[11] R. Basnet, C. Sun, H. Wu, H. T. Nguyen, F. E. Rougieux, D. Macdonald, *J. Appl. Phys.* **2018**, *124*, 243101.
[12] A. A. Istratov, T. Buonassisi, R. McDonald, A. Smith, R. Schindler, J. Rand, J. P. Kalejs, E. R. Weber, *J. Appl. Phys.* **2003**, *94*, 6552.
[13] D. Macdonald, A. Cuevas, A. Kinomura, Y. Nakano, L. Geerligs, *J. Appl. Phys.* **2005**, *97*, 033523.
[14] G. Stokkan, D. S. Marisa, R. Søndenå, M. Juel, A. Autruffe, K. Adamczyk, H. V. Skarstad, K. E. Ekstrøm, M. S. Wiig, C. C. You, *Phys. Status Solidi A* **2017**, *214*, 1700319.
[15] A. Liu, C. Sun, H. C. Sio, X. Zhang, H. Jin, D. Macdonald, *J. Appl. Phys.* **2019**, *125*, 043103.
[16] A. Liu, C. Sun, V. Markevich, A. Peaker, J. D. Murphy, D. Macdonald, *J. Appl. Phys.* **2016**, *120*, 193103.
[17] D. Macdonald, T. Roth, P. N. Deenapanray, K. Bothe, P. Pohl, J. Schmidt, *J. Appl. Phys.* **2005**, *98*, 083509.
[18] C. Sun, F. E. Rougieux, D. Macdonald, *J. Appl. Phys.* **2014**, *115*, 214907.
[19] D. Macdonald, L. Geerligs, A. Azzizi, *J. Appl. Phys.* **2004**, *95*, 1021.
[20] D. Macdonald, J. Tan, T. Trupke, *J. Appl. Phys.* **2008**, *103*, 073710.
[21] K. Mishra, *Appl. Phys. Lett.* **1996**, *68*, 3281.
[22] A. Liu, D. Macdonald, *Appl. Phys. Lett.* **2017**, *110*, 191604.
[23] R. Ghoshtagore, *J. Appl. Phys.* **1969**, *40*, 4374.
[24] D. Gupta, K. Vieregge, K. Srikrishnan, *Appl. Phys. Lett.* **1992**, *61*, 2178.
[25] I. Guerrero, V. Parra, T. Carballo, A. Black, M. Miranda, D. Cancillo, B. Moralejo, J. Jiménez, J. F. Lelièvre, C. del Cañizo, *Prog. Photovoltaics: Res. Appl.* **2014**, *22*, 923.
[26] Z. Liu, V. Vähänissi, H. S. Laine, M. Lindeberg, M. Yli-Koski, H. Savin, *Adv. Electron. Mater.* **2017**, *3*, 1600435.
[27] D. Macdonald, A. Cuevas, A. Kinomura, Y. Nakano, in *Conf. Record of the Twenty-Ninth IEEE Photovoltaic Specialists Conf.*, **2002**, pp. 285–288.